



*Original Article*

## Low temperature synthesized indium tin oxide nanowires

Tula Jutarosaga<sup>1</sup>, Steven M. Smith<sup>2</sup> and Yong Liang<sup>2</sup>

<sup>1</sup>Department of Physics, Faculty of Science,  
King Mongkut's University of Technology Thonburi, Bangkok, Thailand.

<sup>2</sup>Physical and Digital Realization Research Laboratory, Motorola Labs,  
2100 E. Elliot Road, Tempe, AZ 85284, U.S.A.

Received 11 August 2008; Accepted 8 December 2008

### Abstract

Directional indium tin oxide (ITO) nanowires were successfully grown on  $\text{SiO}_2/\text{Si}$  at temperatures ranging from approximately 640°C to 800°C and pressure of about 300 mtorr using  $\text{SnO}$  and  $\text{In}$  powders. The results show that growth temperature strongly affects the morphology and composition of ITO nanostructures. The X-ray diffraction indicates the presence of both cubic  $\text{In}_2\text{O}_3$  and tetragonal  $\text{SnO}_2$  phases in ITO nanowires. Energy dispersive X-ray spectroscopy shows that the atomic ratio of  $\text{Sn}/\text{In}$  decreases with the increase of growth temperature. The observed particles at the tip of the nanowires indicate that the growth of these nanowires is facilitated by the catalyst-assisted vapor-liquid-solid growth mechanism.

**Keywords:** indium tin oxide, nanowires, vapor-liquid-solid growth mechanism, nanostructure materials

### 1. Introduction

Wide band gap oxide materials, such as  $\text{SnO}_2$ ,  $\text{In}_2\text{O}_3$ , and  $\text{ZnO}$ , have many important roles in electronic devices due to their unique properties: high transmission in the visible range and controllable conductivity. Research on these materials has been done mostly in the form of thin films (2-D structure) and nanoparticles (0-D), whereas relatively less research has been focused on the 1-D materials and their doping properties. Improving the conductivity of 1-D materials through doping is a critical step towards successful utilization of these materials for a number of electronic device applications. Undoped  $\text{SnO}_2$ , Sn-doped  $\text{In}_2\text{O}_3$ , and In-doped  $\text{SnO}_2$  attracted interests from many research groups (Chen *et al.*, 2004; Lee *et al.*, 2004; Li *et al.*, 2005; Wang *et al.*, 2005; Zheng *et al.*, 2005; Luo *et al.*, 2006; Shukla *et al.*, 2006; Wan *et al.*, 2006; Xue *et al.*, 2006; Ellis *et al.*, 2007).

To synthesize these materials, the vapor-liquid-solid (VLS) technique, first proposed by Wagner and Ellis in 1964, has been so far the most widely used method for nanowire growth. Table 1 summarized previously reported data of  $\text{SnO}_2$  and indium tin oxide (ITO) nanostructures. Combinations of  $\text{Sn}$ ,  $\text{SnO}$ ,  $\text{In}$ ,  $\text{In}_2\text{O}_3$ , and carbon have been used to synthesize the ITO nanostructures. The growth temperature of those oxide nanowires was lowered by mixing  $\text{SnO}_2$  and/or  $\text{In}_2\text{O}_3$  source materials with carbon. This method has been known as the carbothermal reduction process. Different kind of metal catalysts such as Au and Pt have been used for nanowire growth. Self catalytic mechanism without any foreign catalyst was also reported. However, the growth temperature of either Sn-doped  $\text{In}_2\text{O}_3$  or In-doped  $\text{SnO}_2$  was reported above 770°C. It was also found that Sn-doped  $\text{In}_2\text{O}_3$  nanowires were not grown well when the temperature reduced to below 750°C (Li *et al.*, 2005). In this work, forest-like indium tin oxide nanostructures were synthesized using the vapor transport technique at a relatively low temperature of 640°C and 720°C. The particles observed at the nanowires tips suggested that the growth of these oxide nanowires was dominated by

\*Corresponding author.

Email address: tula.jut@kmutt.ac.th

Table 1. Previously reported tin oxide and ITO nanostructures

Authors	Source materials	Catalyst	Growth T (°C)	Structure
Lee <i>et al.</i> , 2004	SnO <sub>2</sub>	-	1380	Rutile SnO <sub>2</sub>
Luo <i>et al.</i> , 2006	Sn	Au	850, 1000	-
Zheng <i>et al.</i> , 2005	SnO	-	850	Rutile SnO <sub>2</sub>
Wang <i>et al.</i> , 2005	SnO <sub>2</sub> + active C	Au	950	Rutile SnO <sub>2</sub>
Xue <i>et al.</i> , 2006	SnO + In <sub>2</sub> O <sub>3</sub> + C	Au	930	Rutile SnO <sub>2</sub>
Shukla <i>et al.</i> , 2006	SnO + In	Pt	800 - 900	Rutile SnO <sub>2</sub>
Wan <i>et al.</i> , 2006	SnO + In	Au	800 - 900	Cubic In <sub>2</sub> O <sub>3</sub>
Li <i>et al.</i> , 2005	SnO + In <sub>2</sub> O <sub>3</sub> + C	Au	770 - 900	Cubic In <sub>2</sub> O <sub>3</sub>
This study	SnO + In	Au	640 - 800	Cubic In <sub>2</sub> O <sub>3</sub>

the VLS growth mechanism.

## 2. Experimental procedures

Synthesis of ITO nanowires was carried out in the horizontal quartz tube furnace. The setup was similar to that previously reported (Shukla *et al.*, 2006). As-deposited Au film was targeted to about 5 nm in thickness. Discontinuous Au particles were obtained on the SiO<sub>2</sub>/Si substrate with the diameter ranging from 5 to 30 nm and the particle density of about  $2 \times 10^{11}$  cm<sup>-2</sup>. SnO powder (99.9%) and In powder (99.9%) were used as the source materials for the ITO nanowire growth. The Au/SiO<sub>2</sub>/Si wafers and the source materials were situated in the furnace with both source materials placed up stream in front of the substrate at the same temperature zone. The pressure was set to approximately 300 mtorr. The growth temperatures of 580°C, 640°C, 720°C, and 800°C were investigated. The temperature was quickly ramped up to the respective set point and held at the set points for 30 minutes. The structures, morphologies, and compositions of as-deposited nanowires were then analyzed using X-ray diffraction (XRD, Siemens D5000 diffractometer) and scanning electron microscopy (FE SEM Hitachi-4500) equipped with an energy dispersive X-ray spectroscopy (EDS) unit.

## 3. Results and Discussion

Figure 1a to d show plane-view SEM micrographs of as-deposited ITO structures synthesized at (a) 580°C, (b) 640°C, (c) 720°C, and 800°C, respectively. At 580°C, about 300 nm long and about 50 nm in diameter defective nanostructures were observed. As shown in the inset, the nanostructures consisted of numerous small crystallites. At 640°C, nanowire-like structures, ~1.5 μm in length and ~100 nm in diameter, were formed on the multifaceted ITO seed layer. The ITO nanowires had defined rectangular facets along the axis but non-uniform diameters. The nanowires were only partially vertically-aligned to the substrate, indicating the underlying ITO seed layer might have affected the growth direction of the nanowires.

At 720°C, the as-deposited materials exhibited wire

structures with a length of about 10 μm (shown in Figure 2) and an average diameter of about 150 nm measured at the middle of the nanowires. Also, branching was observed on some nanowires. The size of particles at the tips of the nanowires was equivalent to or slightly smaller than the nanowire's diameter. This might be because Au diffused into the ITO nanowires. As the nanowire grew, the Au alloy particle became smaller. It is well-known that the catalyst size controls the diameter of the nanowires. As a result, the

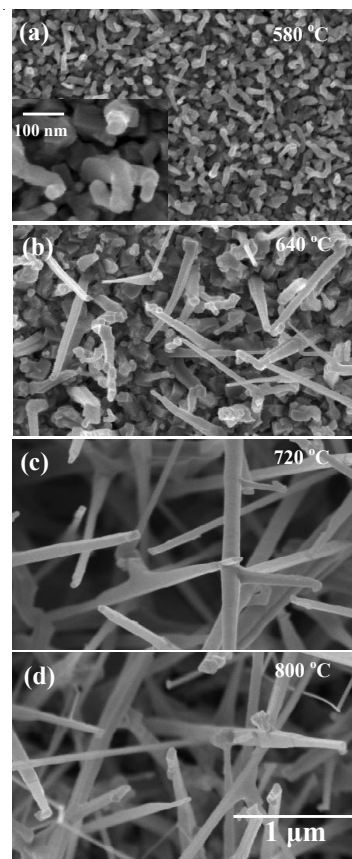


Figure 1. Plane-view scanning electron microscope images of as-deposited ITO structures synthesised at (a) 580°C, (b) 640°C, (c) 720°C, and (d) 800°C.

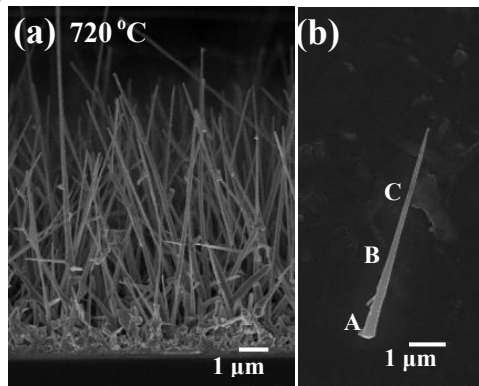


Figure 2. Cross-sectional scanning electron microscope images of (a) as-deposited ITO nanowire forest on  $\text{SiO}_2/\text{Si}$  wafer and (b) individual nanowire synthesized at 720°C.

diameter of the nanowires decreases from the base to the tip. The estimated density of these nanowires was about  $4 \times 10^8 \text{ cm}^{-2}$ . At 800°C, the nanowires similar to those synthesized at 720°C were observed. However, the overall height was slightly shorter than the sample synthesized at 720°C. As the temperature increases, the mass transport increases causing the increase of nanowire growth rate. However, the decrease of the nanowire height at 800°C might be due to the decompositions of the synthesized nanowires as a result of low oxygen partial pressure in the system.

The density, height, and diameter of the nanostructures are summarized in Table 2. The table shows that the estimated density of nanowires decreases from  $\sim 1 \times 10^{10} \text{ cm}^{-2}$  to  $\sim 4 \times 10^8 \text{ cm}^{-2}$ , while the diameter increases from  $\sim 50 \text{ nm}$  to  $\sim 150 \text{ nm}$  with increasing growth temperature from 540°C to 800°C. The estimated aspect ratio, defined as the ratio of the nanowire length to its diameter, increases from  $\sim 6$  to about  $\sim 70$  as the temperature increasing from 540°C to 720°C.

Figure 2a shows an example of a cross-sectional SEM micrograph of ITO nanowires synthesized at 720°C. The presence of the multifaceted ITO seed layer close to the bottom of the oxide layers might have played an important role in controlling the alignment of this nanowire forest. A typical nanowire is shown in Figure 2b. The image suggests that the nanowire diameter decreases from the base to the tip, and that there is a particle at the tip of the nanowire. At the deposition temperature, the Au nanoparticles could form a liquid alloy with the vaporized materials. Sn and In could

Table 2. Summary of particle density, height, and diameter of nanowires

Temperature (°C)	Particle density ( $\text{cm}^{-2}$ )	Height ( $\mu\text{m}$ )	Diameter (nm)
560	$1 \times 10^{10}$	0.3	50
640	$7 \times 10^8$	1.5	100
720	$4 \times 10^8$	10	150
800	$4 \times 10^8$	7	150

be dissolved into the melts and form a Sn-In-Au ternary alloy. When the alloy becomes supersaturated with the presence of  $\text{O}_2$ , nanostructure materials can be precipitated from that alloy. This suggests that the nanowire growth followed the VLS mechanism (Wagner and Ellis, 1964).

Figure 3 shows an example of an EDS spectrum of the ITO nanowire forests synthesized at 720°C. In, Sn, and O are present in the spectrum. The XPS spectrum (not shown) also confirmed the presence of In, Sn, and O. The EDS spectrum further indicated that the Sn/In ratio were relatively uniform along the nanowires, ranging from 0.6, 0.6, and 0.5 from point A to point B and C, in Figure 2b respectively. However, the Sn/In ratio decreased from about 2.1 to about 0.3 as the growth temperature increased from 580°C to 800°C (Figure 4). At low synthesis temperature, In may alloy with Sn. The melting point of the In-Sn alloy is lower than pure Sn at all compositions and lower than pure In when the alloy contains  $<\sim 62$  at. % of Sn. This may cause the increase of the evaporation of Sn atoms. At 800°C, the vapor pressure of In is about 1,000 times of that of Sn. As the temperature increases, the higher vapor of In compared to that of Sn might play an important role in the decrease of the Sn/In ratio.

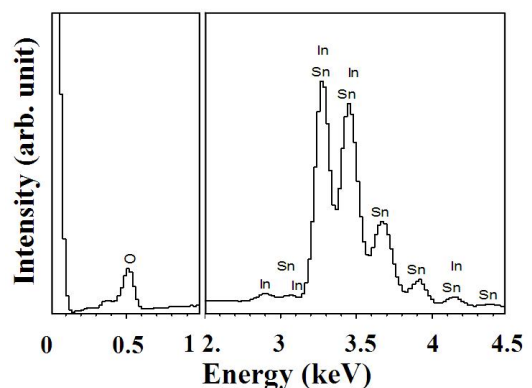


Figure 3. An example of an energy dispersive X-ray spectroscopy spectrum of the as-deposited indium tin oxide nanowire forest synthesized at 720°C.

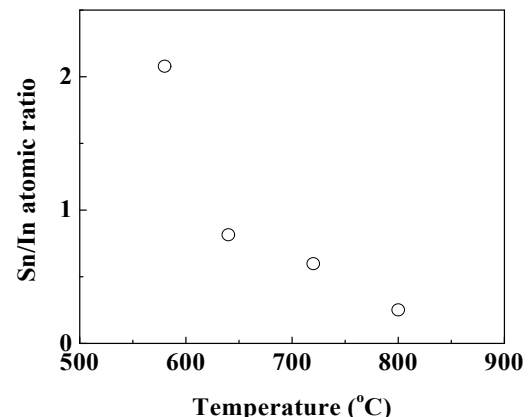


Figure 4. Relationship between Sn/In atomic ratio and growth temperature.

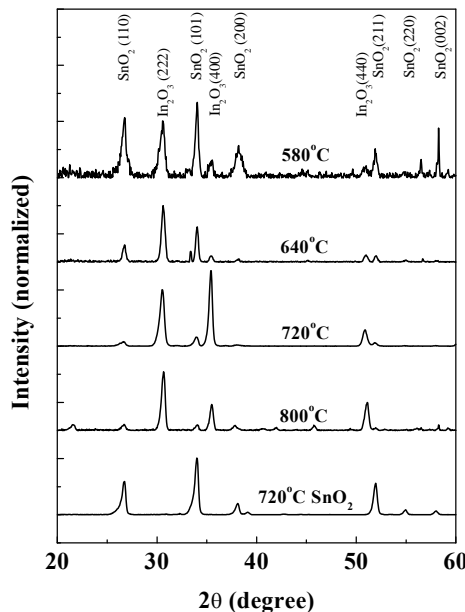


Figure 5. A typical X-ray diffraction spectrum of as-deposited indium tin oxide nanostructures synthesized at 580°C, 640°C, 720°C, and 800°C. Undoped SnO<sub>2</sub> nanowires synthesized at 720°C is added for reference.

Figure 5 shows the XRD spectra of ITO nanowires as a function of the growth temperature. (222), (440), and (400) peaks correspond to In<sub>2</sub>O<sub>3</sub> cubic phase (JCPDS #6-0416), while (110) and (101) peaks correspond to tetragonal Cassiterite SnO<sub>2</sub> (JCPDS #21-1250). The curves were normalized on the (222) peaks of cubic In<sub>2</sub>O<sub>3</sub>. The XRD curve of the undoped SnO<sub>2</sub> nanowires synthesized at 720°C was added for the comparison purpose. The XRD parameters are summarized and shown in Table 3. Due to the presence of both cubic In<sub>2</sub>O<sub>3</sub> and tetragonal Cassiterite SnO<sub>2</sub> phase, Sn-doped In<sub>2</sub>O<sub>3</sub> and In-doped SnO<sub>2</sub> nanowires might be both present in this sample. At 720°C, the highest intensity of (400) was obtained as well as the highest (400)/(222) ratio with 1.33. This ratio reduced to less than 0.44 at other temperatures. In the case of the cubic In<sub>2</sub>O<sub>3</sub> peaks, there was no significant change of the peak positions of both (222) and (400) peaks. However, the full width at half maximum (FWHM) of both (222) and (400) peaks decreased as the growth temperature increased. This suggested that there was an improvement of

Table 3. X-ray diffraction (XRD) peak positions, full width at half maximum (FWHM), and ratio of (222) and (400) peaks

T(°C)	(222) peak		(400) peak		(400)/(222)
	FWHM	Position	FWHM	Position	
580	0.55°	30.57°	0.40°	35.56°	0.31
640	0.43°	30.61°	0.39°	35.44°	0.11
720	0.51°	30.52°	0.38°	35.41°	1.33
800	0.43°	30.64°	0.37°	35.50°	0.44

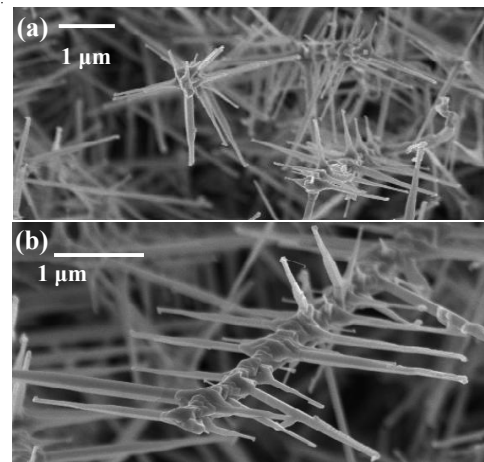


Figure 6. Plan-view scanning electron microscope images of re-deposited indium tin oxide nanowire forest on SiO<sub>2</sub>/Si wafer synthesized at 720°C.

the crystallinity of the ITO nanowires as the temperature increased. From JCPDS #6-0416 cubic In<sub>2</sub>O<sub>3</sub>, the (400)/(222) of the randomly oriented In<sub>2</sub>O<sub>3</sub> intensity ratio was 0.3. The ratio of 1.33 at 720°C indicated that a directional growth of In<sub>2</sub>O<sub>3</sub> nanowires. The directional growth at this temperature might be due to (400) plane texturing the underlying In<sub>2</sub>O<sub>3</sub>-based seed layer close to the substrate, which was also observed in the Sn-doped In<sub>2</sub>O<sub>3</sub> films (Maruyama *et al.*, 1991).

Figure 6a and b show SEM micrographs of re-growth nanowires. These nanowires were obtained by the re-deposition of Au nanoparticles on the as-deposited nanowires and then processed through the similar growth procedures. The majority of the samples had a four-fold symmetry as shown in Figure 6a. The re-grown nanowires were perpendicular to the backbone nanowire with a rectangular cross section. In some cases, the branched nanowires showed an asymmetry, which differed from the four-fold symmetry. For example, a two-fold symmetry was observed as shown in Figure 6b, where the branches attached only to the larger sides of the rectangular backbone nanowires.

Our data showed that the growth of the ITO nanowires was dictated by the VLS mechanism. The growth was likely initiated by the liquid alloy droplet of Au, In, and Sn, and precipitation occurred when the droplet became supersaturated with the source materials. We also found that Au was critical since no nanowire growth was observed without the Au catalyst. Another important parameter was found to be the presence of trace amount of O<sub>2</sub> in the system, which helped to oxidize the In and to convert SnO to SnO<sub>2</sub> during the ITO nanowire growth.

#### 4. Conclusions

In conclusion, high-aspect-ratio ITO nanowires were successfully grown on SiO<sub>2</sub>/Si through a VLS mechanism at

relative low temperature of about 720°C using SnO and In powders as precursor materials. The EDS indicated that the Sn/In atomic ratio was uniform along the growth direction. The XRD indicated both cubic  $In_2O_3$  and tetragonal Cassiterite  $SnO_2$  phases. The particles at the tip of the nanowires suggested that the growth was facilitated by the catalyst-assisted VLS growth mechanism.

### Acknowledgment

The authors would like to thank the Physical and Digital Realization Research Laboratory (PDR), Motorola Labs, for financial support.

### References

Lee, J., Sim, S., Min, B. Cho, K, Kim, S., and Kim, S. 2004. Structural and optoelectronic properties of  $SnO_2$  nanowires synthesized from ball-milled  $SnO_2$  powders. *Journal of Crystal Growth*. 267, 145-149.

Luo, S., Fan, J., Liu, W., Zhang, M., Song, Z., Lin, C., Wu, X., and K., C. 2006. Synthesis and low-temperature photoluminescence properties of  $SnO_2$  nanowires and nanobelts, *Nanotechnology*. 17, 1695-1699.

Zheng, C., Wan, J., Cheng, Y., Cu, D., and Zhan, Y. 2005. Preparation of  $SnO_2$  nanowires synthesized by vapor-solid mode and its growth mechanism. *Int. International Journal of Modern Physics B*. 19, 2811-2816.

Wang, B., Yang, B. H., Wang, C. X., and Yang, G. W. 2005. Nanostructures and self-catalyzed growth of  $SnO_2$ . *Journal of Applied Physics*. 98, 73520-1-73520-5.

Xue, X. Y., Chen, Y. J., Liu, Y. G., Shi, S. L., Wang, Y. G., and Wang T. H. 2006. Synthesis and ethanol sensing properties of indium-doped tin oxide nanowires. *Applied Physics Letters*. 88, 201907-1 - 2017907-3.

Shukla, S., Venkatachalamapathy, V., and Seal, S. 2006. Thermal evaporation processing of nano and submicron tin oxide rods. *Journal of Physical Chemistry B*. 110, 11210-11216.

Wan, Q., Feng, P., Wang, T. H. 2006. Vertically aligned tin-doped indium oxide nanowire arrays: Epitaxial growth and electron field emission properties. *Applied Physics Letters* 89. 123102-1-123102-3.

Li, S. Y., Lee, C. Y., Lin, P., and Tseng, T. Y. 2005. Low temperature synthesized Sn doped indium oxide nanowires. *Nanotechnology* 16. 451-457.

Chen Y. Q., Jiang, J., Wang, B., and Hou, J. G. 2004. Synthesis of tin-doped indium oxide nanowires by self-catalytic VLS growth. *Journal of Physics D: Applied Physics*. 37, 3319-3322.

Wagner, R. S., and Ellis, W. C. 1964. Vapor-liquid liquified-solid mechanism of single crystal growth. *Applied Physics Letters*. 4, 89-90.

Maruyama, T. and Fukui, K. 1991. Indium tin oxide thin films prepared by chemical vapour deposition. *Thin solid films*. 203, 297-302.

Ellis, M., Jutarosaga, T., Smith, S.M., Yong, L., Coll, B., Wei, Y., and Seraphin, S. 2007 Growth and Characterization of Crystalline Tin Oxide Nanostructures. *Proceeding Microscopy and Microanalysis*. 13, 682CD - 683CD.